

Hepatocyte Growth Factor Attenuates Liver Fibrosis Induced by Bile Duct Ligation

Jing-Lin Xia, Chunsun Dai,
George K. Michalopoulos, and Youhua Liu

Division of Cellular and Molecular Pathology, Department of Pathology, University of Pittsburgh School of Medicine, Pittsburgh, Pennsylvania

Hepatic fibrosis is a common outcome of a variety of chronic liver diseases. Here we evaluated the therapeutic efficacy of hepatocyte growth factor (HGF) on liver fibrosis induced by bile duct ligation (BDL) and investigated potential mechanisms. Mice underwent BDL, followed by intravenous injections of naked HGF expression plasmid or control vector. HGF gene therapy markedly ameliorated hepatic fibrotic lesions, as demonstrated by reduced α -smooth muscle actin (α SMA) expression, attenuated deposition of type I and type III collagen, and normalized total hydroxyproline content. HGF also suppressed transforming growth factor- β 1 (TGF- β 1) expression. Interestingly, colocalization of α SMA and cytokeratin-19 in bile duct epithelium was observed, suggesting the possibility of biliary epithelial to myofibroblast transition after BDL. Cells that were still positive for cytokeratin-19 but actively producing type I collagen were found in the biliary epithelia and periductal region. Laminin staining revealed an impaired basement membrane of the bile duct epithelium in diseased liver. These lesions were largely prevented by HGF administration. *In vitro*, treatment of human biliary epithelial cells with TGF- β 1 induced α SMA and fibronectin expression and suppressed cytokeratin-19. HGF abolished the phenotypic conversion of biliary epithelial cells induced by TGF- β 1. These results suggest that HGF ameliorates hepatic biliary fibrosis in part by blocking bile duct epithelial to mesenchymal transition. (*Am J Pathol* 2006, 168:1500–1512; DOI: 10.2353/ajpath.2006.050747)

Liver fibrosis/cirrhosis is a common end-result of a wide variety of chronic hepatic diseases following diverse types of injurious insult, such as viral infection and alcoholic, drug, or chemical toxicity. It is often associated with

severe morbidity and significant mortality, eventually resulting in the necessity of liver transplantation.¹ The pathogenesis of liver cirrhosis is characterized by the excess production and deposition of extracellular matrix components that lead to tissue scarring and the destruction of normal hepatic parenchyma.^{2,3} Several lines of evidence indicate that α -smooth muscle actin (α SMA)-positive myofibroblasts are the principal effector cells that are primarily responsible for the overproduction of matrix components in fibrotic liver.² Therefore, delineation of the originality and mechanism of activation of the matrix-producing myofibroblast cells may be indispensable for designing rational therapeutic strategies for effective treatment of liver cirrhosis.

In an effort to define the origin and regulation of myofibroblast activation in hepatic fibrosis, we have sought to investigate the pathogenesis of liver fibrosis in experimental animals induced by bile duct ligation (BDL). Hepatic fibrosis induced by BDL is unique in that the primary pathological lesions occur surrounding the bile duct epithelium. The maneuver of BDL introduces biomechanical stress to biliary epithelium and initially triggers the compensatory proliferation and expansion of biliary epithelial cells (BECs).^{4,5} Following this epithelial mitogenic phase, chronic obstruction of bile duct causes massive activation of myofibroblasts in the periductal region and ultimately results in biliary fibrosis/cirrhosis. There is little doubt that myofibroblast activation is one of the key steps that initiate fibrotic lesions in this model. However, the exact origin of these periductal myofibroblasts remains largely unknown, although it is often presumed that they are from local activation of residential fibroblasts or hepatic stellate cells.

Supported by National Institutes of Health grants DK054922, DK061408, and DK064005.

J.-L.X. and C.D. contributed equally to this work.

Accepted for publication January 24, 2006.

Current address of J.-L.X.: Liver Cancer Institute, Zhongshan Hospital, Department of Medicine, Shanghai Medical College, Fudan University, Shanghai, China.

Address reprint requests to Youhua Liu, Ph.D., Department of Pathology, University of Pittsburgh, S-405 Biomedical Science Tower, 200 Lothrop Street, Pittsburgh, PA 15261. E-mail: liuy@upmc.edu.

Recent studies from other organs have suggested that matrix-producing myofibroblasts may also come from epithelial cells through a phenotypic conversion known as epithelial to mesenchymal transition (EMT).^{6,7} For instance, in the obstructive nephropathy induced by unilateral ureteral obstruction, kidney tubular epithelial cells can undergo phenotypic transition via EMT to give rise to matrix-producing myofibroblasts.^{8,9} Furthermore, blockade of this transition by hepatocyte growth factor (HGF) prevents renal interstitial fibrosis.¹⁰ These findings highlight that mature epithelial cells in adult animals may possess an incredible plasticity, with the ability to transform into myofibroblasts in response to chronic injury. Such epithelial cell plasticity is also observable in the liver.^{11,12} Numerous studies have shown that, under certain conditions, BECs may give rise to hepatic oval cells, which in turn may become mature hepatocytes.^{13–16} Vice versa, in the conditions of the organoid cultures or in vivo, hepatocytes can undergo phenotypic transition into BECs.^{17,18} Thus BECs and hepatocytes appear to be reciprocally exchangeable. Along this line, we hypothesized that, in pathological circumstances, BECs may transform into α SMA-positive, matrix-producing myofibroblasts as well.

HGF, a multifunctional protein that was originally characterized as a potent mitogen for mature hepatocytes,¹⁹ has emerged as a potent anti-fibrotic cytokine that prevents tissue fibrosis in various organs, including the liver.^{20–23} It has been shown that HGF specifically preserves renal tubular epithelial cell phenotype by inhibiting epithelial to myofibroblast transition both in vitro and in vivo.¹⁰ Therefore, in this study, we evaluated the therapeutic potential of HGF in blocking hepatic fibrosis induced by DBL and explored the possibility of the biliary epithelial to myofibroblast transition in vivo and in vitro.

Materials and Methods

Cell Culture and Treatment

Human intrahepatic biliary epithelial cells (HIBEpiCs) and epithelial cell medium were purchased from ScienCell Research Laboratories (San Diego, CA). HIBEpiCs were nonimmortalized cells isolated from human liver tissue, and the purity of these cells was almost 100% based on their positive staining for cytokeratin-19. The HIBEpiCs were seeded on six-well culture plates to approximately 60% to 70% confluence in complete medium containing 2% fetal bovine serum for 16 hours and then changed to serum-free medium after washing twice with medium. Recombinant human transforming growth factor (TGF)- β 1 (R & D Systems, Minneapolis, MN) was added to the culture at a final concentration of 2 ng/ml. Recombinant human HGF (R & D Systems) was also added at the same time at the concentration of 40 ng/ml, except when otherwise indicated. The cells were typically incubated for 72 hours after addition of cytokines, except when noted otherwise, before harvesting and subjecting to Western blot and immunofluorescence staining as described below.

Animals

Male CD-1 mice that weighed approximately between 18 and 21 g were obtained from Harlan Sprague-Dawley (Indianapolis, IN). They were housed in the animal facilities of the University of Pittsburgh Medical Center with free access to food and water. Mice were randomly assigned to three groups: 1) sham control; 2) BDL followed by injection with empty vector pcDNA3; or 3) BDL followed by injection with HGF expression plasmid. BDL was performed as described elsewhere.⁴ Briefly, under methoxyflurane anesthesia, the common bile duct was double-ligated using 4-0 silk after a midline abdominal incision. Sham-operated mice had their common bile duct exposed and manipulated but not ligated. Starting on the day of surgery, mice were administered human HGF cDNA plasmid under the control of cytomegalovirus (CMV) promoter (pCMV-HGF) through tail-vein injections at a concentration of 1 mg/kg body weight every other week (biweekly), as described previously.^{24,25} Control mice received biweekly injections of the same volume of empty vector (pcDNA3). Animals were sacrificed at 4 and 12 weeks after BDL ($n = 4–6$). At the time of sacrifice, liver tissues were collected for histology and immunohistochemical studies, as well as for mRNA and protein analyses.

Biochemical Measurement of Hepatic Hydroxyproline Content

Total hepatic hydroxyproline level at different time points after BDL was determined in the hydrolysates of liver samples.²⁶ Briefly, precisely weighed liver tissue samples (30 to 40 mg) were homogenized in distilled H₂O. The homogenates were hydrolyzed in 10 N HCl by incubation at 110°C for 18 hours. The hydrolysates were dried by speed vacuum centrifugation over 3 to 5 hours and redissolved in a buffer containing 0.2 mol/L citric acid, 0.2 mol/L glacial acetic acid, 0.4 mol/L sodium acetate, and 0.85 mol/L sodium hydroxide, pH 6.0. Hydroxyproline levels in the hydrolysates were biochemically measured according to the procedures previously described.^{26,27}

Histology and Immunostaining

Liver sections from paraffin-embedded tissues were prepared at 3- μ m thickness using a routine procedure. Sections were stained with hematoxylin/eosin for general histology. Another set of sections was stained using the Masson's trichrome staining method for identifying interstitial collagen by blue color. A computer-aided morphometric analysis was used for quantitatively determining the area of fibrosis, as reported previously.²⁸ Briefly, a series of digital images was captured from the Masson's trichrome-stained sections. The areas of fibrosis were measured by using morphometric analysis software (MetaMorph; Universal Imaging Corp., Downingtown, PA).²⁹ The percentage of the fibrotic area per total liver area was calculated based on each individual animal.

Immunofluorescence and immunohistochemical staining were performed on liver tissue cryosections and paraffin-embedded sections, respectively. All immunostainings were performed by using the Vector M.O.M. Immunodetection kit according to the procedures specified by the manufacturer (Vector Laboratories, Burlingame, CA). The primary antibodies used for staining were as follows: goat polyclonal antibodies against type I and type III collagen (Southern Biotechnology Associates, Birmingham, AL) (dilution 1:50); anti-TGF- β 1 (sc-146), anti-TGF- β type I receptor (sc-398), and anti-heat shock protein 47 (Santa Cruz Biotechnology Inc., Santa Cruz, CA) (dilution 1:100); mouse monoclonal anti- α SMA antibody (clone 1A4, dilution 1:50) and monoclonal antibodies for cytokeratin-19 (DakoCytomation, Carpinteria, CA, dilution 1:20); monoclonal anti-fibronectin (clone 10, dilution 1:1000; BD Transduction Laboratories, San Diego, CA); and anti-laminin (Chemicon Inc., Temecula, CA, dilution 1:100). Double immunofluorescence staining was performed on paraffin-embedded sections (3 μ m) or cryosections (4 μ m) by using different combinations of antibodies. For instance, for double staining for cytokeratin-19 and α SMA, liver sections were first incubated with monoclonal anti-cytokeratin-19 for 1 hour at room temperature. Biotin-conjugated anti-mouse IgG1 (A85-1; BD Pharmingen, San Diego, CA) was then added, and the mixture was incubated for 30 minutes. The staining reaction was developed with cyanine Cy3-conjugated streptavidin (Jackson ImmunoResearch Laboratories, West Grove, PA) for 30 minutes. The sections were then incubated with anti- α SMA (isotype IgG2a; Dako, Carpinteria, CA) for 1 hour, followed by incubation with fluorescein isothiocyanate anti-mouse IgG2a (R19-15, BD Pharmingen, dilution 1:100) for 30 minutes. As a negative control, the primary antibody was replaced with nonimmune IgG, and no staining occurred.

Immunofluorescence staining of HIBEpCs was performed using an established procedure. Briefly, control or cytokine-treated HIBEpCs cultured on coverslips were fixed with cold methanol:acetone (1:1) for 10 minutes on ice and blocked with 20% normal donkey serum in phosphate-buffered saline buffer for 30 minutes at room temperature and then incubated with the specific primary antibodies described above. To visualize the primary antibodies, cells were stained with fluorescein isothiocyanate- or cyanine Cy3-conjugated secondary antibodies (Jackson ImmunoResearch Laboratories, Inc.). Cells were counterstained with 4',6-diamidino-2-phenylindole, HCl to visualize the nuclei. Stained cells were viewed under a Nikon Eclipse E600 Epi-fluorescence microscope equipped with a digital camera (Melville, NY).

Western Blot Analysis

Liver samples were homogenized by using a Polytron homogenizer in radioimmune precipitation assay lysis buffer (1% Nonidet P-40, 0.1% sodium dodecyl sulfate (SDS), 100 μ g/ml phenylmethylsulfonyl fluoride, 0.5% sodium deoxycholate, 1 mmol/L sodium orthovanadate, 2 μ g/ml aprotinin, 2 μ g/ml antipain, and 2 μ g/ml leupeptin

in phosphate-buffered saline) on ice. The supernatants were collected after centrifugation at 13,000 $\times g$ at 4°C for 20 minutes. Protein concentration was determined using a bicinchoninic acid protein assay kit (Sigma), and whole tissue lysates were mixed with an equal amount 2 \times SDS loading buffer (125 mmol/L Tris-HCl, 4% SDS, 20% glycerol, 100 mmol/L dithiothreitol, and 0.2% bromophenol blue), as described previously.^{10,24} HIBEpCs and cytokine-treated cells were lysed with SDS sample buffer. Samples were heated at 100°C for 5 to 10 minutes before loading and were separated on 10% SDS-polyacrylamide gels. The proteins were electrotransferred to a nitrocellulose membrane (Amersham Biosciences, Piscataway, NJ) in transfer buffer containing 48 mmol/L Tris-HCl, 39 mmol/L glycine, 0.037% SDS, and 20% methanol at 4°C for 1 hour. Nonspecific binding to the membrane was blocked for 1 hour at room temperature with 5% nonfat milk in TBS buffer (20 mmol/L Tris-HCl, 150 mmol/L NaCl, and 0.1% Tween 20). The membranes were then incubated for 16 hours at 4°C with various primary antibodies in blocking buffer containing 5% milk at the dilutions specified by the manufacturers, followed by incubation with horseradish peroxidase-conjugated secondary antibody (Bio-Rad, Hercules, CA) for 1 hour in 5% nonfat milk dissolved in Tris-buffered saline. Membranes were then washed with Tris-buffered saline buffer, and the signals were visualized using the enhanced chemiluminescence system (ECL, Amersham Biosciences).

Determination of Tissue TGF- β 1 Levels by Reverse Transcription-Polymerase Chain Reaction

Total RNA was isolated from liver samples by using Ultraspec RNA isolation kit according to the instructions specified by the manufacturer (Biotecx Laboratories, Houston, TX). The first strand cDNA was synthesized by using a Reverse Transcription System (Promega, Madison, WI) with random primers at 42°C for 30 minutes. Polymerase chain reaction (PCR) was performed using a standard PCR kit on 1- μ l aliquots of cDNA and HotStar-Taq polymerase (Qiagen Inc., Valencia, CA) with specific primer pairs for rat TGF- β 1 and β -actin. The sequences of the primers were as follows: TGF- β 1, 5'-GCAACATGTGGAACTCTACCAGAA-3' (sense) and 5'-GACGTCAA-AAGACAGCCACTCA-3' (antisense); β -actin, 5'-AGGC-ATCCTCACCCTGAAGTA-3' (sense) and 5'-CACACG-CAGCTCATTGTAGA-3' (antisense). The PCR protocol consisted of 35 (for TGF- β 1) or 30 (for actin) cycles at 94°C for 1 minute, 55°C for 1 minute, and 72°C for 1.5 minutes, followed by a final extension step at 72°C for 7 minutes. PCR products were size-fractionated on agarose gels and detected by ethidium bromide staining.

Statistical Analyses

Animals were randomly assigned to control and treatment groups. All data were expressed as mean \pm SEM. For Western blot analysis, quantitation was performed by

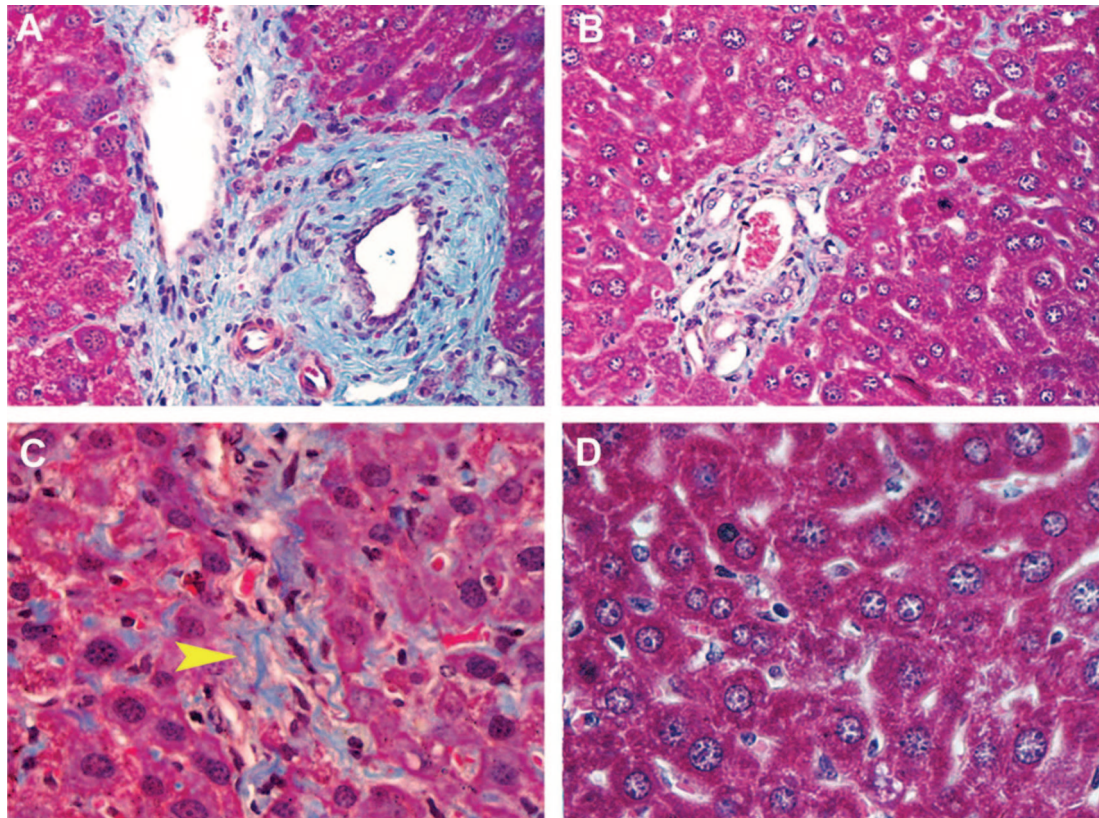


Figure 1. HGF gene therapy attenuates liver fibrosis induced by BDL. Masson's trichrome staining of liver tissue sections from pcDNA3- (A and C) and pCMV-HGF-treated (B and D) mice at 12 weeks after BDL. Extensive peribiliary (A) and interstitial collagen (C) staining was noticeable in liver sections of the mice injected with pcDNA3. Significantly less hepatic collagen staining was observed in pCMV-HGF-treated mice (B and D).

scanning and determination of the intensities of the hybridization signals. Statistical analyses of the data were performed by Student's *t*-test using SigmaStat software (Jandel Scientific, San Rafael, CA). Values of $P < 0.05$ were considered significant.

Results

HGF Suppresses Hepatic Fibrosis Induced by Bile Duct Ligation

To assess the potential effect of exogenous HGF on liver fibrosis, mice were injected through the tail vein with human HGF expression plasmid (pCMV-HGF) or control vector pcDNA3 every other week after common BDL. Our earlier studies have shown that substantial HGF transgene expression was detected in the liver by using this simple gene transfer approach.²⁴ Figure 1 shows representative micrographs of the Masson's trichrome staining of liver tissue sections at 12 weeks after BDL. In mice treated with control pcDNA3 vector, extensive peribiliary (Figure 1A) and interstitial (Figure 1C) collagen deposition was evident, as shown by positive Masson's trichrome staining. However, delivery of HGF gene largely inhibited hepatic collagen accumulation after BDL (Figure 1). Collagen staining was much weaker in the enlarged periductal area (Figure 1B), and essentially no collagen accumulation was found in liver interstitium after

HGF treatment (Figure 1D). A computer-aided morphometric analysis revealed that the area of fibrosis in the liver sections at 12 weeks after BDL was reduced by 74% after pCMV-HGF administration, when compared with the pcDNA3 controls.

To quantitatively evaluate the therapeutic efficacy of HGF on hepatic fibrosis induced by BDL, we determined the hydroxyproline content in the hydrolysates extracted from liver tissue by using biochemical methods. This assay is based on the observation that essentially all of the hydroxyproline in animal tissues is exclusively found in collagen.²⁷ As shown in Figure 2A, the hydroxyproline content was progressively increased in the liver extracts at 4 and 12 weeks after BDL, suggesting increased hepatic fibrosis. However, exogenous HGF substantially reduced the hydroxyproline levels in the liver tissue extracts at different time points, suggesting that HGF is capable of protecting the liver from the development of fibrotic lesions after BDL.

We further examined the accumulation and deposition of the specific extracellular matrix components by immunofluorescence staining. As demonstrated in Figure 2 (B and D), liver sections at 12 weeks after BDL displayed stronger staining for type I and type III collagen, respectively. Consistent with the hydroxyproline assay (Figure 2A), delivery of HGF gene largely blocked hepatic type I and type III collagen deposition in the peribiliary region (Figure 2, C and E).

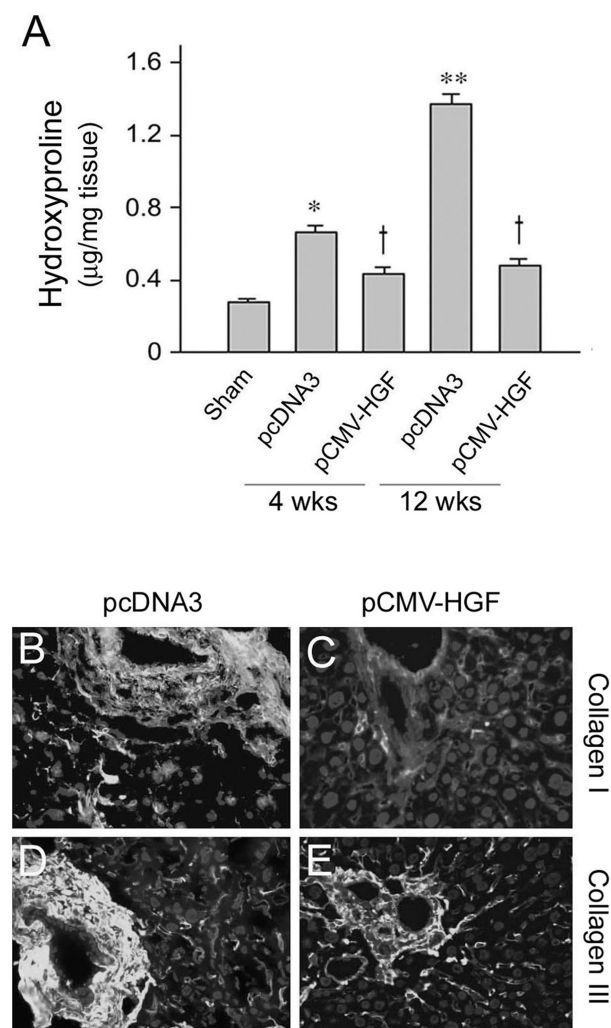


Figure 2. HGF reduces hepatic hydroxyproline content and suppresses type I and type III collagen deposition. **A:** Total tissue hydroxyproline content was determined by biochemical assay. Data were expressed as micrograms of hydroxyproline per milligram of tissue and presented as mean \pm SEM ($n = 4-6$). *, $P < 0.05$ versus sham; **, $P < 0.01$ versus sham; †, $P < 0.05$ versus pcDNA3 control. **B-E:** Representative micrographs showed the deposition of type I (**B** and **C**) and type III (**D** and **E**) collagen in the portal tract region of liver sections. **B** and **D:** pcDNA3; **C** and **E:** pCMV-HGF.

HGF Inhibits TGF- β 1 Expression Induced by BDL

Because TGF- β 1 is a fibrogenic cytokine that is believed to play a central role in regulating tissue fibrosis,^{30,31} we next investigated the effect of exogenous HGF on hepatic TGF- β 1 expression after BDL. As presented in Figure 3A, BDL induced a dramatic increase in hepatic TGF- β 1 gene expression, as determined by reverse transcription-PCR analyses. The steady-state levels of TGF- β 1 mRNA in the liver at 12 weeks after BDL were increased by more than 10-fold, compared to the sham controls (Figure 3B). However, exogenous HGF markedly suppressed hepatic TGF- β 1 mRNA abundance. Figure 3B shows the quantitative determination of the relative TGF- β 1 mRNA abundance in different groups. We also examined TGF- β 1 protein expression in the liver by using immunohistochemical staining. As shown in Figure 3D, TGF- β 1 was

predominantly localized in the biliary epithelium at 12 weeks after BDL. Strong staining for TGF- β 1 was also observed in the periductal region (Figure 3D). Consistent with mRNA expression, TGF- β 1 protein level was extremely low in normal liver (Figure 3C), and exogenous HGF largely suppressed its induction after BDL (Figure 3E). These results are consistent with the notion that biliary epithelial cells are the major source of hepatic TGF- β 1 after BDL.

The expression of TGF- β type I receptor (T β R-I) was also examined in the liver at different time points after BDL. As shown in Figure 3F, neither BDL nor exogenous HGF significantly altered hepatic T β R-I expression at 4 weeks after BDL, as illustrated by Western blot. The T β R-I level appeared to marginally increase at 12 weeks after BDL, whereas HGF suppressed its expression toward the baseline level (Figure 3G).

Immunohistochemical staining revealed that T β R-I protein was predominantly localized in the hepatic bile duct epithelium in both sham and BDL mice. The slight increase in hepatic T β R-I abundance after BDL (Figure 3G) was likely a result of the increased number of biliary epithelial cells, rather than increased expression per cell. Weak staining for the T β R-I protein was also observed in hepatocytes (Figure 3, H-J).

HGF Blocks Myofibroblast Activation in Vivo

Because α SMA-positive myofibroblasts are the effector cells that are primarily responsible for the overproduction of extracellular matrix at pathogenic conditions, we sought to investigate the hepatic myofibroblast activation after BDL. Figure 4 demonstrates the levels of hepatic α SMA protein, the molecular hallmark of myofibroblasts, in sham and BDL mice at different times. Compared with sham controls, α SMA expression in the bile duct-ligated liver at 4 (Figure 4A) and 12 weeks (Figure 4B) was markedly increased, suggesting activation of the hepatic myofibroblasts following BDL-induced injury. However, the induction of α SMA in the diseased liver was largely blocked by intravenous administrations of the HGF gene (Figure 4).

We next examined hepatic myofibroblast activation after BDL by using immunofluorescence staining. In the portal triads of normal liver, hepatic arteriole, adjacent to bile duct, was stained positively for α SMA protein, whereas the bile duct and surrounding area were completely α SMA-negative (Figure 4E). The staining for α SMA was dramatically increased in bile duct-ligated liver. Surprisingly, in addition to the peribiliary region in which α SMA-positive cells were observed, strong α SMA staining was also found in enlarged and/or proliferated biliary epithelia (Figure 4G). To confirm the epithelial origin of α SMA-positive cells, we used double immunofluorescence staining for biliary epithelial marker cytokeratin-19 (red) and α SMA (green). Figure 4H demonstrates clear colocalization of cytokeratin-19 and myofibroblast marker α SMA in biliary epithelial cells at 12 weeks after BDL. Exogenous HGF, however, prevented the coexpression of cytokeratin-19 and α SMA in biliary epithelium (Figure 4K).

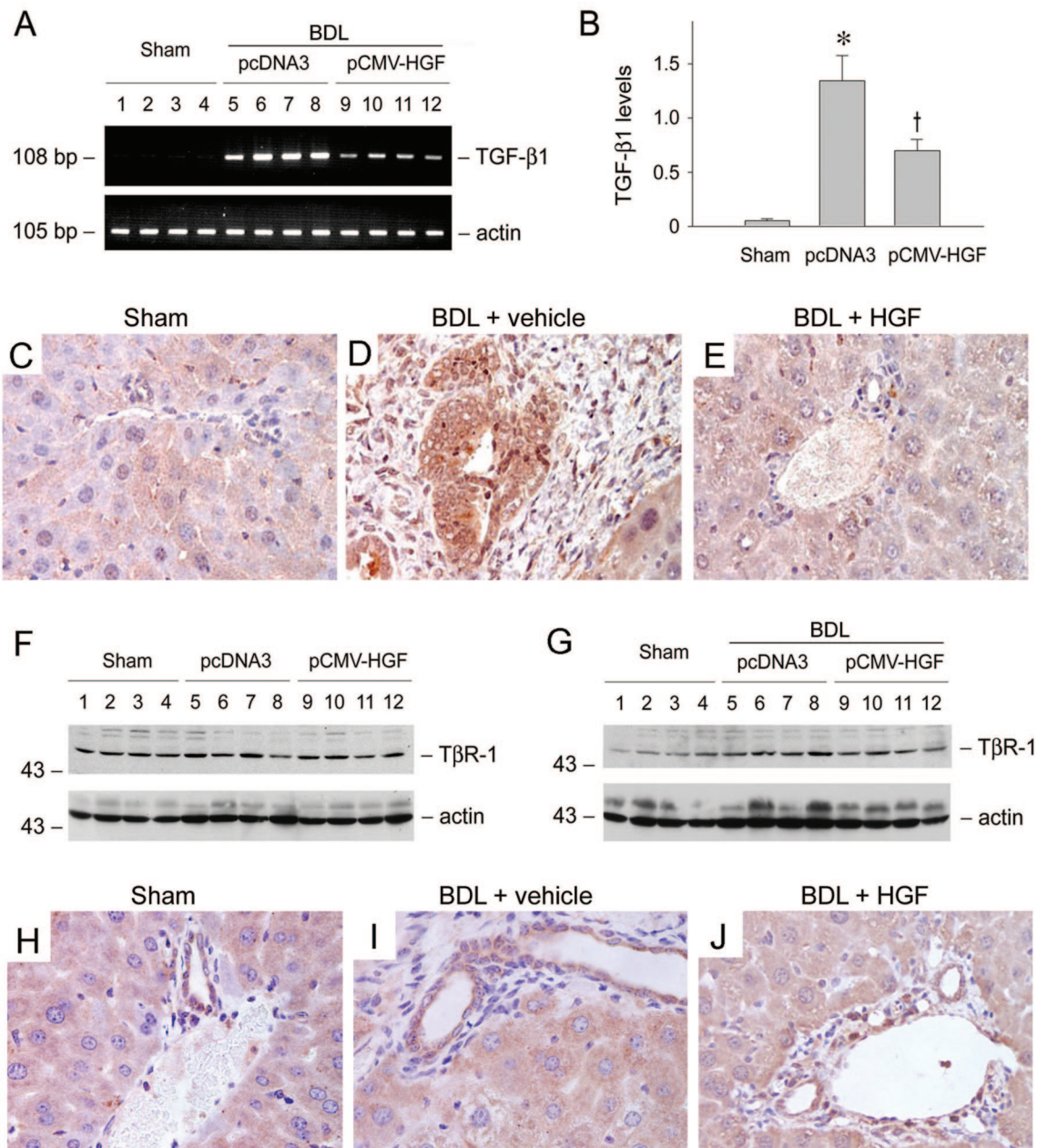


Figure 3. HGF inhibits hepatic TGF-β1 expression. **A:** Reverse transcription-PCR showed an inhibitory effect of HGF on hepatic TGF-β1 expression induced by BDL. The mRNA levels of hepatic TGF-β1 were determined by reverse transcription-PCR at 12 weeks after BDL. The numbers 1 through 12 indicate each individual animal. **B:** Graphic presentation of the relative abundance of TGF-β1 after normalization with actin in various groups as indicated. *, $P < 0.01$ versus sham control; †, $P < 0.05$ versus pcDNA3 control. **C–E:** Representative micrographs showed the localization of TGF-β1 by immunohistochemical staining in sham control (**C**) and BDL mice treated with either pcDNA3 (**D**) or pCMV-HGF (**E**). Strong staining for TGF-β1 was observed in bile duct epithelium, as well as in periductal fibroblast cells in the liver at 12 weeks after BDL (**D**). **F** and **G:** Western blot analyses showed hepatic TGF-β1 type I receptor (TβR-I) abundance at 4 (**F**) and 12 weeks (**G**) after BDL. Liver homogenates were probed with antibodies against TβR-I and actin, respectively. **H–J:** Representative micrographs showed the localization of TβR-I by immunohistochemical staining in sham control (**H**) and BDL mice treated with either pcDNA3 (**I**) or pCMV-HGF (**J**). There was strong immunostaining for TβR-I in bile duct epithelium in all three groups. Weak staining for TβR-I was also noticeable in hepatocytes.

Similar results were obtained when liver sections were immunohistochemically stained for αSMA (Figure 4, L–N). The αSMA-positive cells were not only observed in the peribiliary region as expected but also found in the bile duct epithelium at 4 (Figure 4L) and 12 weeks (Figure 4M) after BDL, respectively; HGF treatment significantly reduced αSMA staining (Figure 4N). These observations imply that BECs may undergo a phenotypic transition into myofibroblasts under patho-

logical conditions and that HGF could protect the biliary epithelia by blocking this phenotypic transition.

Evidence for Biliary Epithelial to Myofibroblast Transition in Vivo

To seek further evidence that BECs can undergo phenotypic conversion into matrix-producing myofibroblasts,

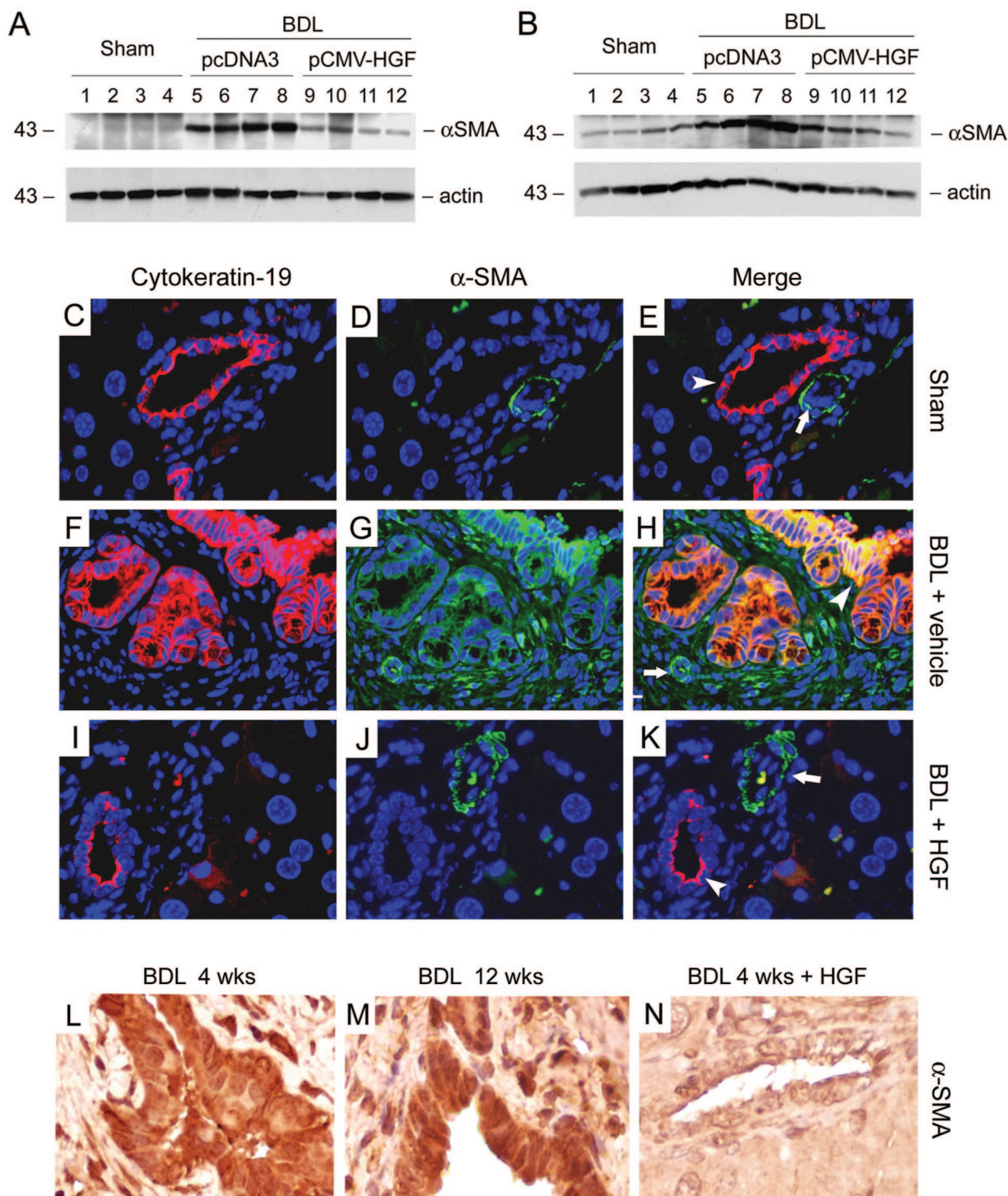


Figure 4. Colocalization of the bile duct epithelial marker cytokeratin-19 and myofibroblast marker αSMA. **A** and **B**: Exogenous HGF inhibited hepatic expression of αSMA after BDL. Western blot analyses showed hepatic αSMA abundance at 4 (**A**) and 12 weeks (**B**) after BDL. Liver homogenates were probed with antibodies against αSMA and actin, respectively. **C–K**: Double immunofluorescence staining showed the localization of cytokeratin-19 (red, left column) and αSMA (green, center column) in the liver sections at 12 weeks after BDL. Merging of cytokeratin-19 and αSMA staining is presented in right column (**E**, **H**, and **K**). **C–E**, sham control; **F–H**, BDL liver injected with pcDNA3; **I–K**, BDL liver injected with pCMV-HGF. **Arrowheads** denote bile duct epithelia. **Arrows** indicate αSMA-positive hepatic arteriole. Colocalization of cytokeratin-19 and αSMA is clearly evident in the bile duct epithelium after ligation (**H**). **L–N**: Immunohistochemical staining showed the localization of αSMA in bile duct epithelium at 4 and 12 weeks after BDL, respectively. **L**, 4 weeks after BDL; **M**, 12 weeks after BDL; **N**, liver injected with pCMV-HGF, 4 weeks after BDL.

we examined the cells that undertook active production of interstitial collagen in the diseased liver at 12 weeks after BDL. Heat-shock protein (hsp) 47, a molecular

chaperone for type I collagen in cells actively engaged in collagen synthesis,^{9,32} was used as a surrogate marker for the identification of the cells with active intracellular

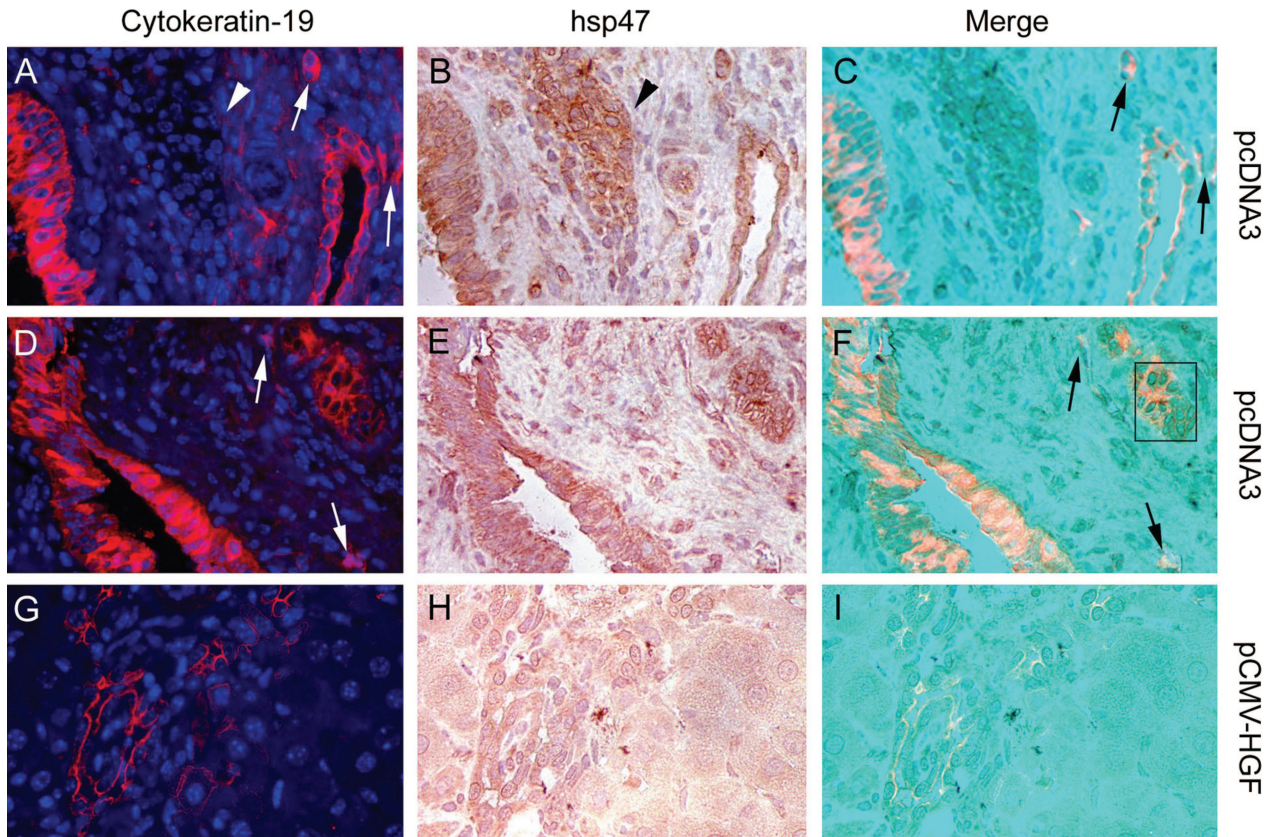


Figure 5. Double immunostaining shows a transition of the bile duct epithelial cells to matrix-producing interstitial cells. Liver sections were prepared from the mice receiving pcDNA3 (A–F) or pCMV-HGF (G–I) injections at 12 weeks after BDL, and stained using antibodies against cytokeratin-19 (red, left column) and hsp47 (brown, middle column). Merging of cytokeratin-19 and hsp47 staining is presented in right column (C, F, and I). **Arrowheads** denote a cluster of cells that retained bile duct epithelial cell appearance, but lost cytokeratin-19, and were hsp47-positive. **Arrows** indicate cytokeratin-19-positive cells that localized in interstitial compartment, with strong staining for hsp47. Boxed area (F) showed a cluster of bile duct epithelial cells that they were all positive for hsp47 staining, but only some of them were still positive for cytokeratin-19.

collagen production. As shown in Figure 5, immunohistochemical staining identified the hsp47-positive cells in hepatic peribiliary region after BDL, presumably being myofibroblasts. Intriguingly, BECs also stained strongly for hsp47 (Figure 5, B and E), suggesting that these cells actively synthesize interstitial type I collagen. The identity of BECs was confirmed by double staining with cytokeratin-19 (red) and hsp47 (brown). Of particular interest, clusters of cells with degenerated epithelial appearance and strong staining for hsp47 were found in the peribiliary region (Figure 5B, arrowhead), and these cells completely lacked the biliary epithelial marker cytokeratin-19 (Figure 5, A and C). In some areas, a fraction of the cell population still retained cytokeratin-19 in clusters of epithelial cells with strong staining for hsp47, whereas other cells within the same cluster had already lost the epithelial marker (Figure 5, D–F). Of note, biliary epithelium-originated cells with positively staining for cytokeratin-19 were frequently seen in the peribiliary region in a scattered fashion. These isolated BECs actively produced interstitial type I collagen as shown by hsp47 staining and displayed assorted shapes and morphological appearances ranging from epithelium-like to spindle-shaped fibroblasts (Figure 5, A–F, arrows). Hence, these observations indicate that BECs contribute to interstitial matrix production and are capable of migrating into the periduc-

tal region and undergoing phenotypic transition via EMT into myofibroblasts. Consistent with amelioration of hepatic fibrosis (Figure 2), treatment with exogenous HGF largely prevented biliary epithelial to myofibroblast transition (Figure 5, G–I).

To determine whether BECs produce type I collagen after chronic injury, as indicated by hsp47 staining, we performed double immunostaining for type I collagen and cytokeratin-19 in liver sections at 12 weeks after BDL. As demonstrated in Figure 6, strong staining for type I collagen was observed in the bile duct epithelium. Double staining with cytokeratin-19 confirmed that BECs produced large amounts of type I collagen (Figure 6D). In the periductal region, scattered BEC clusters also displayed positive type I collagen staining (Figure 6A, arrowhead). Consistently, exogenous HGF suppressed BECs to produce type I collagen. No or little type I collagen staining was found in the bile duct epithelium after HGF administration (Figure 6, E–H). Hence, these results essentially recapitulate the hsp47 staining (Figure 5) and indicate that BECs and their derivatives are active producers of interstitial type I collagen after chronic injury.

BECs are normally surrounded and physically confined by an underlying basement membrane (BM), a structure primarily composed of laminin and type IV collagen. To understand how the BECs migrate into the

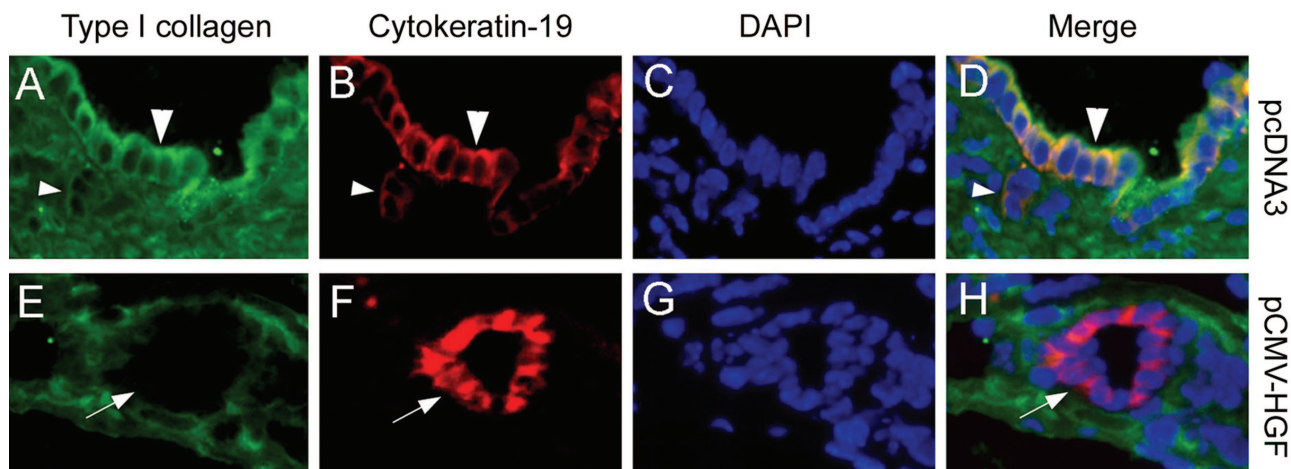


Figure 6. Double immunostaining shows the expression of type I collagen in bile duct epithelial cells after BDL. Liver sections were prepared from the mice receiving pcDNA3 (**A–D**) or pCMV-HGF (**E–H**) injections at 12 weeks after BDL and stained using antibodies against type I collagen (**A** and **E**) and cytokeratin-19 (**B** and **F**). Nuclear staining with 4',6-diamidino-2-phenylindole, HCl was shown (**C** and **G**). Merging of the images was presented (**D** and **H**). **Arrowheads** denote the bile duct epithelial cells that stained positively for type I collagen. **Arrows** indicate the bile duct epithelial cells that were negative for type I collagen in mice receiving pCMV-HGF injections.

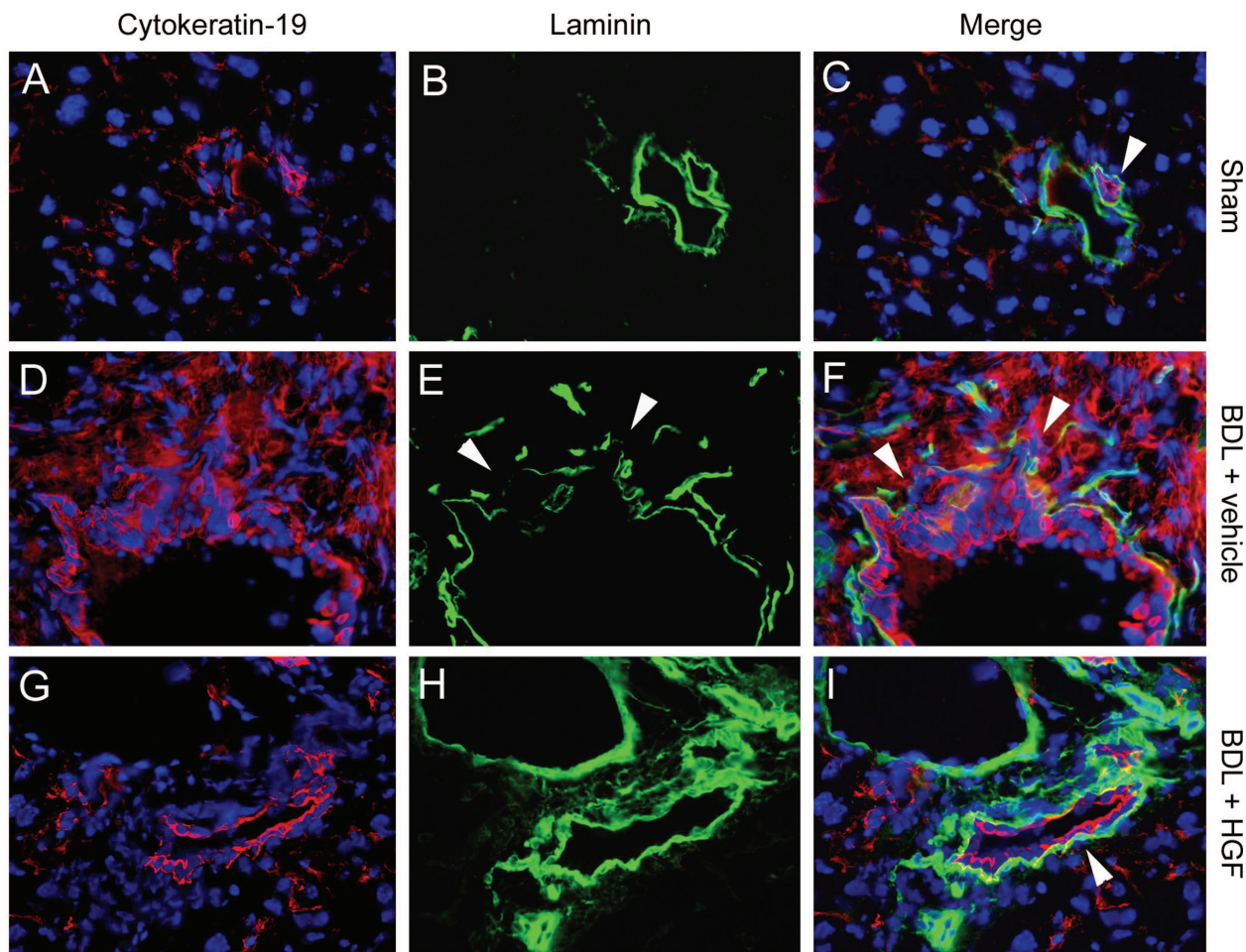


Figure 7. Double immunostaining demonstrates the impairment of the bile duct basement membrane and the migration of cytokeratin-19-positive cells after BDL. Liver sections were prepared from sham control (**A–C**), BDL mice injected with pcDNA3 (**D–F**) or pCMV-HGF (**G–I**) and stained using antibodies against cytokeratin-19 (red, left column) and laminin (green, middle column). Merging of cytokeratin-19 and laminin staining is presented in right column (**C**, **F**, and **I**). The integrity of bile duct basement membrane, as shown by laminin staining (**arrowheads**), was clearly impaired after ligation. The cytokeratin-19-positive epithelial cells could easily migrate into interstitial compartment through broken basement membrane (**arrowheads** in **E** and **F**).

periductal region by escaping the confinement of the epithelial BM, we next examined the integrity of BM by immunostaining for its major component laminin. As shown in Figure 7, both the bile duct and its adjacent portal vein are surrounded by laminin-positive BM. However, the integrity of BM was severely impaired in the diseased liver at 12 weeks after BDL (Figure 7E). BM was clearly broken and often contained big gaps that allowed the BECs to easily escape. Double staining for laminin (green) and cytokeratin-19 (red) demonstrated that the cytokeratin-19-positive BECs could readily move into the periductal region through the broken BM (Figure 7F). However, delivery of exogenous HGF gene largely preserved the BM integrity of the bile duct epithelium (Figure 7I).

HGF Blocks TGF- β 1-mediated Biliary Epithelial to Myofibroblast Transition in Vitro

To provide direct evidence for biliary epithelial to myofibroblast transition, human intrahepatic BECs were used as a model system to investigate the phenotypic conversion of the BECs in vitro. We found that when human BECs were incubated with TGF- β 1, a well characterized fibrogenic cytokine whose expression is markedly induced in bile duct epithelium after BDL (Figure 3), *de novo* expression of the myofibroblast marker α SMA was observable in a time-dependent fashion (Figure 8A), suggesting that TGF- β 1 is able to induce BECs to undergo phenotypic conversion. These cells following TGF- β 1 treatment also started to produce interstitial matrix component fibronectin (Figure 8A). Meanwhile, the expression of biliary epithelial marker cytokeratin-19 was progressively suppressed after the TGF- β 1 treatment (Figure 8, A and B). Therefore, cultured BECs after TGF- β 1 treatment may undergo a series of phenotypic changes, including lose of an epithelial marker, gain of the myofibroblast marker α SMA, and production of large amounts of interstitial matrix, consistent with the notion of epithelial to myofibroblast transition.

Figure 9 demonstrates that HGF could block TGF- β 1-mediated biliary EMT in vitro. Simultaneous incubation of the BECs with HGF significantly abrogated the α SMA and fibronectin expression induced by TGF- β 1. Furthermore, HGF completely restored the cytokeratin-19 expression that was suppressed by TGF- β 1 in BECs (Figure 9A). The inhibitory effect elicited by HGF on biliary EMT was dose-dependent (Figure 9B). At a concentration of 40 ng/ml, HGF largely abolished α SMA and fibronectin expression induced by 2 ng/ml of TGF- β 1. Similar results were obtained by using indirect immunofluorescence staining (Figure 9). We also determined the cell numbers with positive staining for α SMA or cytokeratin-19 after different treatments, respectively. In the control group, there were 62% of the BECs stained positively for cytokeratin-19 (Figure 9K), but all cells were negative for α SMA (Figure 9C). After TGF- β 1 treatment for 3 days, 79% of the cell population exhibited α SMA-positive staining (Figure 9D), whereas the number of cytokeratin-19-positive cells was reduced to <1% (Figure 9L). Treatment with HGF alone

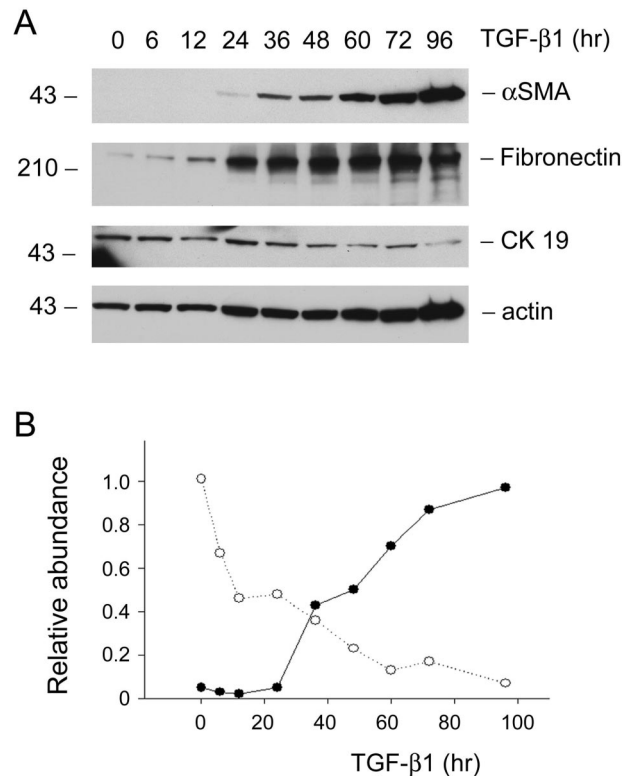


Figure 8. TGF- β 1 induces bile duct EMT. HIBEPiCs were incubated with 2 ng/ml of TGF- β 1 in serum-free medium for various periods of time as indicated. Whole cell lysates were immunoblotted with antibodies against α SMA, fibronectin, cytokeratin-19, and actin, respectively. **A:** Representative Western blots. **B:** Graphic presentation of the relative abundance of α SMA and cytokeratin 19 after normalization with actin.

(Figure 9, E, I, and M) or HGF plus TGF- β 1 (Figure 9, F, J, and N) displayed a staining pattern similar to the controls. Hence, HGF is able to preserve the differentiated phenotype of BECs by blocking TGF- β 1-mediated epithelial to myofibroblast transition in vitro.

Discussion

It has been long recognized that the activation of the α SMA-positive, matrix-producing myofibroblasts is one of the decisive events in tissue fibrogenesis after chronic injury. Despite this, the origin of these cells in the fibrotic tissues remained largely undefined. They are often presumed to be derived from hepatic stellate cells or/and residential fibroblasts.^{33–36} In this study, we have shown that, in the biliary fibrosis induced by BDL, periductal myofibroblasts may also be generated from the bile duct epithelium through epithelial to mesenchymal phenotypic transition. This conclusion is supported by numerous accounts of observation. First, BECs coexpress both the epithelial marker cytokeratin-19 and the myofibroblast marker α SMA after BDL, indicating the presence of a transitional stage between two phenotypes. Second, single cells or loosely organized small cell clusters still positive for cytokeratin-19 are scattered in the periductal region. Vice versa, cell clusters with BEC morphology but without cytokeratin-19 are clearly present. Third, BECs at

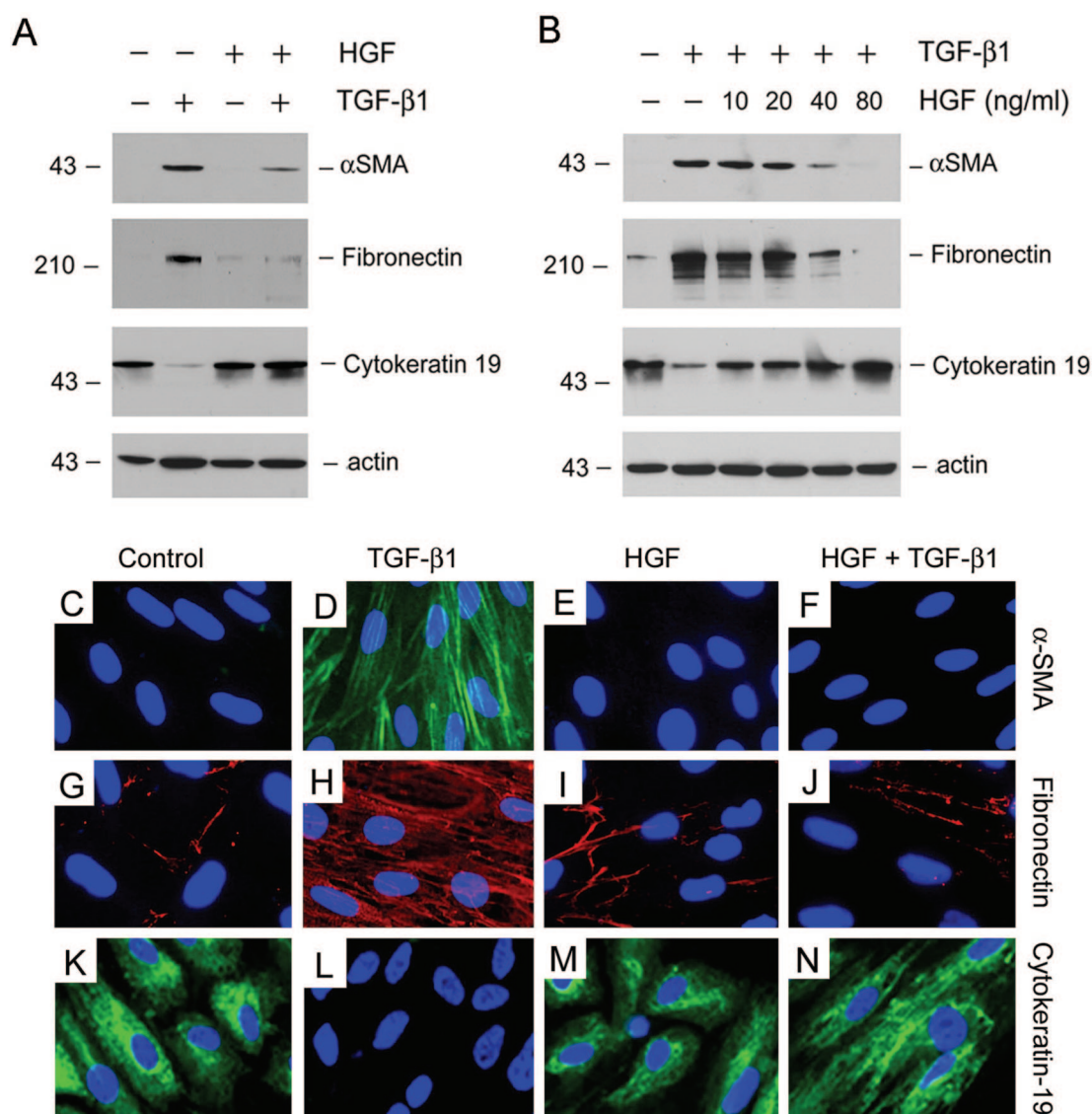


Figure 9. HGF blocks TGF-β1-mediated bile duct EMT. **A:** HIBEpCs were incubated without (control) or with 2 ng/ml TGF-β1, 40 ng/ml HGF, or both for 3 days. Whole cell lysates were immunoblotted with antibodies against αSMA, fibronectin, cytokeratin-19, and actin, respectively. **B:** Western blot demonstrates that HGF blocks TGF-β1-mediated bile duct EMT in a dose-dependent fashion. Cells were treated with a fixed dose of TGF-β1 (2 ng/ml) and an increasing amount of HGF as indicated. **C–N:** Representative micrographs show the immunofluorescence staining for αSMA (**C–F**), fibronectin (**G–J**), and cytokeratin 19 (**K–N**) in bile duct epithelial cells after various treatments. Control (**C**, **G**, and **K**); TGF-β1, (**D**, **H**, and **L**); HGF (**E**, **I**, and **M**); and TGF-β1 plus HGF (**F**, **J**, and **N**).

various transitional stages actively produce interstitial type I collagen in the fibrotic environment. Fourth, phenotypic conversion of the bile duct epithelium can be recapitulated in cultured human BECs in vitro following incubation with fibrogenic TGF-β1. Finally, blockade of biliary EMT by HGF prevents hepatic myofibroblast activation and biliary fibrosis. Collectively, these findings raise the possibility that BECs have the capacity to undergo phenotypic transition into αSMA-positive, matrix-producing myofibroblasts under pathological conditions. Such mesenchymal transition of BECs may represent a potential avenue to generate myofibroblasts in response to fibrogenic cues, thereby playing a role in the pathogenesis of hepatic fibrosis/cirrhosis.

Phenotypic transition of epithelial cells into myofibroblasts in a fibrotic environment has been documented in other organs.^{8,9} Ample studies have shown that kidney

tubular epithelial cells transform into matrix-producing fibroblasts in a wide variety of chronic kidney diseases in both experimental animals and patients.^{7,37,38} In unilateral ureteral obstructed kidney, a large proportion of the interstitial fibroblasts (approximately 36%) are actually originated from tubular epithelium via EMT.⁹ Likewise, selective blockade of tubular EMT in tPA^{-/-} mice dramatically attenuates renal interstitial fibrosis.³⁹ The obstructive nephropathy model induced by ureteral ligation in many ways is quite similar to BDL in this study. Both ureteral and bile duct ligations cause biomechanical stress and injury to epithelium, which is followed by an inflammatory response, compensatory epithelial cell proliferation, up-regulation of fibrogenic cytokine TGF-β1 expression, and myofibroblast activation.^{4,40} In this regard, it is not surprising that the BECs are also capable of undergoing phenotypic transition to give rise to the ma-

trix-producing myofibroblast cells after BDL. Hence, phenotypic conversion via EMT may be a common pathway leading to myofibroblast activation in fibrotic tissues in different parenchymal organs.

BDL is a unique experimental animal model of hepatic fibrosis/cirrhosis. In humans, several clinical conditions can lead to biliary fibrosis, including primary sclerosing cholangitis and extrahepatic biliary atresia.⁴ It remains to be determined whether phenotypic transition via EMT also plays a role in the pathogenesis of liver cirrhosis caused by other etiologies, such as viral infection and alcoholic and chemical toxicity. Myofibroblast activation is also a predominant pathological finding in the fibrotic liver induced by these injurious stimuli; however, they are generally considered to be derived from the activation of hepatic stellate cells.^{33,41,42} Whether other cell types, such as hepatocytes via EMT, contribute to the myofibroblast pool in a diseased state is an intriguing question. In view of the findings that hepatocytes and BECs are exchangeable,^{13,17} it is possible that hepatocytes may also undergo phenotypic transition via EMT to become myofibroblasts to participate in the development of hepatic fibrosis. Indeed, *in vitro* studies have shown that cultured neonatal rat hepatocytes are capable of undergoing EMT at certain conditions.^{43,44} The process of hepatocyte EMT involves the loss of their typical differentiation markers, the acquisition of a migrating morphology, and a change in the expression of the intermediate filament protein cytokeratin to vimentin.^{43–45}

Although BECs can transform to myofibroblasts and apparently migrate into the periductal region via the impaired basement membrane, it is conceivable that the periductal myofibroblasts may originate from other sources as well.^{35,36} We envision that hepatic stellate cells, residential fibroblasts, BECs, and perhaps bone marrow-derived cells, all contribute to the periductal myofibroblast pool after BDL. In this regard, myofibroblasts may display tremendous heterogeneity in terms of their originality. Such heterogeneity is also illustrated by a recent observation that α -SMA expression and collagen production are not always linked in the BDL model.⁴⁶ Along this line, it is likely that the anti-fibrotic effects of HGF may be mediated by other mechanisms, including blockade of the myofibroblast activation from hepatic stellate cells, peribiliary fibroblasts, or/and bone marrow-derived cells, besides inhibition of biliary EMT. At this stage, it remains to be determined the relative contributions of the diverse sources to myofibroblast pool, as well as their importance in biliary fibrogenesis. This issue cannot be addressed in the present study, because the epithelial cell markers such as cytokeratin-19 would gradually diminish along the lines of the acquisition of mesenchymal features. New techniques to specifically tag BECs *in vivo* with cell markers that are expressed independently of differentiated status are needed to determine their destination. Nonetheless, in light of the observation that most BECs obtained α -SMA, the hallmark of myofibroblasts, in the biliary epithelium after BDL *in vivo* (Figure 4) and in cultured BECs after TGF- β 1 incubation *in vitro* (Figure 9), it is reasonable to speculate that biliary

EMT may play a significant role in generating myofibroblasts in the disease state.

What triggers BECs to undergo biliary EMT after BDL remains to be determined *in vivo*. However, TGF- β 1 appears to be a plausible candidate that may play a central role in mediating biliary EMT. This notion is supported by several pieces of evidence. First, the expression of TGF- β 1 is markedly induced in the liver after BDL. BECs express abundant TGF- β 1 and its receptors, suggesting that they are the natural sources as well as the targets of this potent fibrogenic cytokine. More importantly, incubation with TGF- β 1 *in vitro* induced BECs to endure a phenotypic conversion. A crucial role of TGF- β 1 signaling in mediating biliary EMT is also consistent with the observations that implicate TGF- β /Smad signaling in the regulation of EMT in other organs. A previous study has indicated that ablation of Smad3 prevents renal tubular EMT after ureteral obstruction in mice.⁴⁷ Similarly, antagonizing Smad signaling with overexpression of Smad transcriptional corepressor SnoN blocks TGF- β 1-mediated EMT in kidney tubular epithelium.⁴⁸ Of note, HGF did not completely inhibit TGF- β 1 expression after BDL *in vivo* (Figure 3), suggesting that alternative actions of HGF may be at work. In harmony with this notion, HGF is found to be able to directly block TGF- β 1 action in cultured BECs (Figure 9). Such dual effects of HGF on TGF- β 1 (both expression and action) would lead to substantial suppression of the fibrogenic actions of TGF- β 1 under diseased conditions.

In summary, this study suggests that HGF acts as a negative regulator of EMT that prevents BECs from undergoing phenotypic transition *in vivo* and *in vitro*. Although the antifibrotic effects of HGF have been recognized, the present study unravels a novel mechanism by which HGF elicits its beneficial action. In this regard, the present study not only underscores that the blockade of EMT is a novel strategy for prevention of fibrotic diseases but also sets a foundation for the rational utilization of HGF in combating hepatic fibrosis/cirrhosis.

References

1. Pinzani M, Rombouts K: Liver fibrosis: from the bench to clinical targets. *Dig Liver Dis* 2004, 36:231–242
2. Albanis E, Friedman SL: Hepatic fibrosis. Pathogenesis and principles of therapy. *Clin Liver Dis* 2001, 5:315–334, v–vi
3. Eng FJ, Friedman SL: Fibrogenesis I. New insights into hepatic stellate cell activation: the simple becomes complex. *Am J Physiol* 2000, 279:G7–G11
4. Ezure T, Sakamoto T, Tsuji H, Lunz JG, third, Murase N, Fung JJ, Demetris AJ: The development and compensation of biliary cirrhosis in interleukin-6-deficient mice. *Am J Pathol* 2000, 156:1627–1639
5. Lunz JG, III, Contrucci S, Ruppert K, Murase N, Fung JJ, Starzl TE, Demetris AJ: Replicative senescence of biliary epithelial cells precedes bile duct loss in chronic liver allograft rejection: increased expression of p21(WAF1/Cip1) as a disease marker and the influence of immunosuppressive drugs. *Am J Pathol* 2001, 158:1379–1390
6. Kalluri R, Neilson EG: Epithelial-mesenchymal transition and its implications for fibrosis. *J Clin Invest* 2003, 112:1776–1784
7. Liu Y: Epithelial to mesenchymal transition in renal fibrogenesis: pathological significance, molecular mechanism, and therapeutic intervention. *J Am Soc Nephrol* 2004, 15:1–12
8. Yang J, Liu Y: Dissection of key events in tubular epithelial to myofi-

- broblast transition and its implications in renal interstitial fibrosis. *Am J Pathol* 2001, 159:1465–1475
9. Iwano M, Plieth D, Danoff TM, Xue C, Okada H, Neilson EG: Evidence that fibroblasts derive from epithelium during tissue fibrosis. *J Clin Invest* 2002, 110:341–350
10. Yang J, Liu Y: Blockage of tubular epithelial to myofibroblast transition by hepatocyte growth factor prevents renal interstitial fibrosis. *J Am Soc Nephrol* 2002, 13:96–107
11. Thorgeirsson SS, Grisham JW: Overview of recent experimental studies on liver stem cells. *Semin Liver Dis* 2003, 23:303–312
12. Hixson DC, Chapman L, McBride A, Faris R, Yang L: Antigenic phenotypes common to rat oval cells, primary hepatocellular carcinomas and developing bile ducts. *Carcinogenesis* 1997, 18:1169–1175
13. Alison M, Golding M, Lalani EN, Nagy P, Thorgeirsson S, Sarraf C: Wholesale hepatocytic differentiation in the rat from ductular oval cells, the progeny of biliary stem cells. *J Hepatol* 1997, 26:343–352
14. Alison MR, Vig P, Russo F, Bigger BW, Amofah E, Themis M, Forbes S: Hepatic stem cells: from inside and outside the liver? *Cell Prolif* 2004, 37:1–21
15. Haque S, Haruna Y, Saito K, Nalesnik MA, Atillasoy E, Thung SN, Gerber MA: Identification of bipotential progenitor cells in human liver regeneration. *Lab Invest* 1996, 75:699–705
16. Sirica AE, Gainey TW, Mumaw VR: Ductular hepatocytes. Evidence for a bile ductular cell origin in furan-treated rats. *Am J Pathol* 1994, 145:375–383
17. Michalopoulos GK, Bowen WC, Mule K, Lopez-Talavera JC, Mars W: Hepatocytes undergo phenotypic transformation to biliary epithelium in organoid cultures. *Hepatology* 2002, 36:278–283
18. Michalopoulos GK, Barua L, Bowen WC: Transdifferentiation of rat hepatocytes into biliary cells after bile duct ligation and toxic biliary injury. *Hepatology* 2005, 41:535–544
19. Michalopoulos GK, DeFrances MC: Liver regeneration. *Science* 1997, 276:60–66
20. Liu Y: Hepatocyte growth factor in kidney fibrosis: therapeutic potential and mechanisms of action. *Am J Physiol Renal Physiol* 2004, 287:F7–F16
21. Matsumoto K, Nakamura T: Hepatocyte growth factor: renotropic role and potential therapeutics for renal diseases. *Kidney Int* 2001, 59:2023–2038
22. Matsuda Y, Matsumoto K, Yamada A, Ichida T, Asakura H, Komoriya Y, Nishiyama E, Nakamura T: Preventive and therapeutic effects in rats of hepatocyte growth factor infusion on liver fibrosis/cirrhosis. *Hepatology* 1997, 26:81–89
23. Ueki T, Kaneda Y, Tsutsui H, Nakanishi K, Sawa Y, Morishita R, Matsumoto K, Nakamura T, Takahashi H, Okamoto E, Fujimoto J: Hepatocyte growth factor gene therapy of liver cirrhosis in rats. *Nat Med* 1999, 5:226–230
24. Yang J, Chen S, Huang L, Michalopoulos GK, Liu Y: Sustained expression of naked plasmid DNA encoding hepatocyte growth factor in mice promotes liver and overall body growth. *Hepatology* 2001, 33:848–859
25. Dai C, Yang J, Liu Y: Single injection of naked plasmid encoding hepatocyte growth factor prevents cell death and ameliorates acute renal failure in mice. *J Am Soc Nephrol* 2002, 13:411–422
26. Yang J, Dai C, Liu Y: Hepatocyte growth factor gene therapy and angiotensin II blockade synergistically attenuate renal interstitial fibrosis in mice. *J Am Soc Nephrol* 2002, 13:2464–2477
27. Kivirikko KI, Laitinen O, Prockop DJ: Modifications of a specific assay for hydroxyproline in urine. *Anal Biochem* 1967, 19:249–255
28. Moal F, Chappard D, Wang J, Vuillemin E, Michalak-Provost S, Rousselet MC, Oberti F, Cales P: Fractal dimension can distinguish models and pharmacological changes in liver fibrosis in rats. *Hepatology* 2002, 36:840–849
29. Dai C, Huh CG, Thorgeirsson SS, Liu Y: β -Cell-specific ablation of the hepatocyte growth factor receptor results in reduced islet size, impaired insulin secretion, and glucose intolerance. *Am J Pathol* 2005, 167:429–436
30. Bissell DM, Roulot D, George J: Transforming growth factor β and the liver. *Hepatology* 2001, 34:859–867
31. George J, Roulot D, Kotliansky VE, Bissell DM: *In vivo* inhibition of rat stellate cell activation by soluble transforming growth factor β type II receptor: a potential new therapy for hepatic fibrosis. *Proc Natl Acad Sci USA* 1999, 96:12719–12724
32. Nicole O, Docagne F, Ali C, Margail I, Carmeliet P, MacKenzie ET, Vivien D, Buisson A: The proteolytic activity of tissue-plasminogen activator enhances NMDA receptor-mediated signaling. *Nat Med* 2001, 7:59–64
33. Safadi R, Friedman SL: Hepatic fibrosis: role of hepatic stellate cell activation. *Med Gen Med* 2002, 4:27
34. Eddy AA: Molecular basis of renal fibrosis. *Pediatr Nephrol* 2000, 15:290–301
35. Kruglov EA, Nathanson RA, Nguyen T, Dranoff JA: Secretion of MCP-1/CCL2 by bile duct epithelia induces myofibroblastic transdifferentiation of portal fibroblasts. *Am J Physiol* 2006, 290:G765–G771
36. Kinnman N, Housset C: Peribiliary myofibroblasts in biliary type liver fibrosis. *Front Biosci* 2002, 7:d496–d503
37. Rastaldi MP, Ferrario F, Giardino L, Dell'Antonio G, Grillo C, Grillo P, Strutz F, Muller GA, Colasanti G, D'Amico G: Epithelial-mesenchymal transition of tubular epithelial cells in human renal biopsies. *Kidney Int* 2002, 62:137–146
38. Liu Y: Renal fibrosis: new insights into the pathogenesis and therapeutics. *Kidney Int* 2006, 69:213–217
39. Yang J, Shultz RW, Mars WM, Wegner RE, Li Y, Dai C, Nejak K, Liu Y: Disruption of tissue-type plasminogen activator gene in mice reduces renal interstitial fibrosis in obstructive nephropathy. *J Clin Invest* 2002, 110:1525–1538
40. Klahr S, Morrissey J: Obstructive nephropathy and renal fibrosis. *Am J Physiol* 2002, 283:F861–F875
41. Wu J, Zern MA: Hepatic stellate cells: a target for the treatment of liver fibrosis. *J Gastroenterol* 2000, 35:665–672
42. Friedman SL: Molecular mechanisms of hepatic fibrosis and principles of therapy. *J Gastroenterol* 1997, 32:424–430
43. Pagan R, Martin I, Llobera M, Vilaro S: Epithelial-mesenchymal transition of cultured rat neonatal hepatocytes is differentially regulated in response to epidermal growth factor and dimethyl sulfoxide. *Hepatology* 1997, 25:598–606
44. Pagan R, Sanchez A, Martin I, Llobera M, Fabregat I, Vilaro S: Effects of growth and differentiation factors on the epithelial-mesenchymal transition in cultured neonatal rat hepatocytes. *J Hepatol* 1999, 31:895–904
45. Valdes F, Alvarez AM, Locascio A, Vega S, Herrera B, Fernandez M, Benito M, Nieto MA, Fabregat I: The epithelial mesenchymal transition confers resistance to the apoptotic effects of transforming growth factor β in fetal rat hepatocytes. *Mol Cancer Res* 2002, 1:68–78
46. Magness ST, Bataller R, Yang L, Brenner DA: A dual reporter gene transgenic mouse demonstrates heterogeneity in hepatic fibrogenic cell populations. *Hepatology* 2004, 40:1151–1159
47. Sato M, Muragaki Y, Saika S, Roberts AB, Ooshima A: Targeted disruption of TGF- β 1/Smad3 signaling protects against renal tubulointerstitial fibrosis induced by unilateral ureteral obstruction. *J Clin Invest* 2003, 112:1486–1494
48. Yang J, Zhang X, Li Y, Liu Y: Down-regulation of Smad transcriptional corepressors SnoN and Ski in the fibrotic kidney: an amplification mechanism for TGF- β 1 signaling. *J Am Soc Nephrol* 2003, 14:3167–3177